Dávid Samu · Péter Erős · Balázs Ujfalussy · Tamás Kiss

Robust path integration in the entorhinal grid cell system with hippocampal feed-back

Abstract Animals are able to update their knowledge about their current position solely by integrating the speed and the direction of their movement, known as path integration. Recent discoveries suggest that grid cells in the medial entorhinal cortex might perform some of the essential underlying computations of path integration. However, a major concern over path integration is that as the measurement of speed and direction is inaccurate, the representation of the position will become increasingly unreliable. In this paper we study how allothetic inputs can be used to continually correct the accumulating error in the path integrator system. We set up the model of a mobile agent equipped with the entorhinal representation of idiothetic (grid cell) and allothetic (visual cells) information and simulated its place learning in a virtual environment. Due to competitive learning a robust hippocampal place code emerges rapidly in the model. At the same time, the hippocampo-entorhinal feed-back connections are modified via Hebbian learning in order to allow hippocampal place cells to influence the attractor dynamics in the entorhinal cortex. We show that the continuous feed-back from the integrated hippocampal place representation is able to stabilize the grid cell code.

Keywords sensor fusion · place representation · learning · noise · error correction

This research was supported by the EU Framework 6 ICEA project (IST 027819).

D. Samu
Department of Biophysics, KFKI Research Institute for Particle and Nuclear Physics of the Hungarian Academy of Sciences

P. Erős
Department of Biophysics, KFKI Research Institute for Particle and Nuclear Physics of the Hungarian Academy of Sciences

B. Ujfalussy
Department of Biophysics, KFKI Research Institute for Particle and Nuclear Physics of the Hungarian Academy of Sciences

T. Kiss
Department of Biophysics, KFKI Research Institute for Particle and Nuclear Physics of the Hungarian Academy of Sciences
Konkoly-Thege út 29 – 33, H-1121, Budapest, Hungary
Tel.: +36-1-392-2222 x3257
Fax: +36-1-392-2742
E-mail: bognor@mail.kfki.hu
URL: http://cneuro.rmki.kfki.hu

1 Introduction

During the course of their evolution animals have developed several types of sensory organs. Information collected by these can be used by the animal to execute several tasks required for its survival. One such task is navigation for which animals at different levels of development use different types of sensory inputs. In rodents these types include auditory, tactile, visual (allothetic) and self-motion (idiothetic) information (Maaswinkel and Whishaw 1999). Integration of these modalities into a unified representation of the environment might serve as the basis for navigation in animals at a high level of phylogenetic development. Electrical recordings from single cells in the rat hippocampus showing highly spatially correlated cell activity (O'Keefe and Dostrovsky 1971), indicated that this structure might be the site of integrated spatial representation in the rat brain (O'Keefe and Nadel 1978). Indeed, the integration of different modalities in the hippocampus is supported by both the anatomy of this structure (Amaral and Witter 1989; Amaral and Lavenex 2006) and the influence of the different types of modalities on the place representation by the hippocampal cells (Wiener et al 1995; Jeffery 2007). For example, on one hand, changing the visual appearance of the testing environment by modifying its shape (Muller and Kubie 1987; Leutgeb et al 2007) or rotating the landmarks supposedly used for self-localization (Jeffery and O'Keefe 1999) would alter the firing pattern of place cells in a way systematically corresponding to changes in the environment. On the other hand, self-motion information has an effect on place cell firing both in the angular (Jeffery and O'Keefe 1999) and in the linear (Gothard et al 1996) domain. Most intriguingly, rats are able to switch back-and-forth between vision and path integration depending on their reliability in case they are in conflict (Jeffery 1998).

Path integration is performed using self-motion information (Etienne and Jeffery 2004), which originates from the visual-flow, the vestibular system, proprioceptive motor copies, etc. Theoretical considerations (McNaughton et al 2006) suggest that path integration in rats, using this multimodal information, is performed in the attractor network of the recently discovered entorhinal grid cell system (Hafting et al 2005), which functions as a preprocessing stage in the generation of the hippocampal place code. These cells found in all layers of the medial entorhinal cortex were (EC) shown to fire on a regular hexagonal lattice, tessellating the space (Hafting et al 2005; Sargolini et al 2007).

Path integration alone, however, can not be used by animals or robots for proper navigation as errors in the measurement of speed and direction increasingly accumulate, and after the animal proceeds a certain distance this error would invalidate self localization. Fortunately, combining allothetic and idiothetic information offers a way to ameliorate path integration and get rid of the harmful noise. There is evidence showing that in humans, when the visual and the self-motion information are in conflict either the visual system resets the self-motion system based on a remembered location of landmarks or the two information are integrated (Nardini et al 2008). Specifically, adults when facing conflicting cues use a weighted average of cues in determining their location, while young children alternated between the use of either information source without combining them. In rats, however, when vision and self-motion are in conflict place cells generally prefer to follow the visual stimulus (Knierim et al 1995; Jeffery 1998; Maaswinkel and Whishaw 1999). Moreover, depending on the precision needed to achieve a goal, animals might swap the different navigation strategies. For example, during homing, hamsters first follow a relatively straight line indicating the use of path integration (Séguinot et al 1993), however, when they get close to their nest, they switch to follow a circular trajectory in a search for familiar (visual) cues (for a review see (Etienne et al 1996; Etienne and Jeffery 2004)).

The exact mechanism of how grid cells and place cells interact with each other to form a robust representation of the environment is still to be elucidated. Building on experimental observations several components of the underlying neural structures have been studied by theoretical tools. The first models explaining the generation of hippocampal place cell activity from visual inputs used the distance from and the bearing to identified landmarks as input to the hippocampus (Zipser 1985; Sharp 1991; Burgess et al 1994; Touretzky and Redish 1996; Barry and Burgess 2007). Hippocampal place cells were activated when the currently perceived scene matched the stored landmark configuration. However, these models require exact object recognition, and representation of distances and angles between objects in the EC. If such a representation is present, place cell activity, i.e. a partitioning of the environment into place fields, emerges from the combination of a Hebbian-like learning between the EC and hippocampal cells and competition among hippocampal place cells (Sharp 1991). Later it was shown (Ujfalussy et al 2008) that similar Hebbian mechanism is able to produce place cell like activity even if the representation of the sensory input is less elaborated.

An other theory proposed by Burgess and O'Keefe (1996) suggests that hippocampal place cell activity is based on the firing of so called boundary vector cells (Barry et al 2006) A neural network model based on this theory was successfully implemented in a mobile robot (Burgess et al 2000), which used real-word inputs: sensory input cells, feeding their output into entorhinal cortical cells, were selective to the distance of a wall in a particular direction. Interestingly, very recently this model was supported by experimental evidence, whereby cells, termed border cells, in the medial EC and adjacent parasubiculum were found to fire when the rat was close to a geometric border of the environment (Solstad et al 2008). These cells might serve to produce a reference frame for location determination and could be used to error correction, when the animal reaches the border, or even more, a corner of the environment. However, the question how the error accumulating in the path integrator while the animal moves from border to border still requires further elaboration.

Here, we ask the question how errors accumulating in path integration is corrected in the entorhino-hippocampal system in a biologically plausible way. Specifically, in the present study we propose a mechanism, which combine path integration via entorhinal grid cells and vision to create a unified representation of the environment by hippocampal place cells. We assume that the projection from CA1 and subiculum to the deep layers of the entorhinal cortex can influence the attractor dynamics in the entorhinal cortex, and that these connections are established through Hebbian learning when the environment is novel. This approach is consistent with the idea proposed by O'Keefe and Burgess (2005), who suggested that a feed-back innervation from hippocampal place cells to entorhinal grid cells facilitates the association of grid cells to sensory inputs and associations between different sets of connected grid cells. Furthermore, we show that these feed-back connections empower the system to correct self-localization errors originating from noisy path integration.

2 Methods

For numerical simulations of the entorhino-hippocampal model, we set up a virtual environment and a simple robot model in the Webots (Michel 2004) mobile robotics simulation software. All physical events happening to the robot (displacing it, turning it, blocking its movement when hitting obstacles), as well as maintaining the communication between the external word and the neural network model via robotic sensors were handled by Webots. To explore its environment, the robot moved forward in a straight line for three time steps, then turned randomly left or right 0.3 radians. A time step in the simulations was 0.125 seconds and the robot's speed was 0.22 meters per second.

The neural model – the whisker cell, local visual cell, grid cell and the place cell models – was run within the robotic simulation using inputs from the robot's sensors. Outputs – firing rates of cells – were saved and processed off-line in the R software environment (R Development Core Team 2007). Control of the robot was not connected to the neural model in any way, the robot moved randomly and sampled the environment.

2.1 Overview of the neural network model

The neural network model consisted of neurons in the barrel cortex, entorhinal cortical grid cells, local visual cells and hippocampal place cells (Fig. 1). Inputs from the external world originated from the robot's sensors and were represented as firing rates in the entorhinal and barrel cortical part of the model. As we intended to study how allothetic information can be used to ameliorate path integration, we used noisy proprioceptive input in the simulations. Error accumulated (Fig. 2 **a**) in the path integrator and invalidated the neural representation of position.

Cortical neurons (the input layer) innervated hippocampal cells via modifiable synapses. Hippocampal cells in turn exhibited spatially correlated firing similar to experimentally observed place cells. In the present model hippocampal cells integrated the three types of modalities represented in the cortical models. We used this integrated place representation to stabilize the spatial firing pattern of grid cells via a feed-back excitation from the hippocampus to grid cells.

In the following sections of the Methods we describe the parts of the model in more detail.

2.2 Inputs of the model

The neural network model receives three types of inputs from the environment (Fig. 2 **b**). First, 20 distance sensors represented by 20 rate models were used to simulate the whisking of rats. Whenever the robot moved close enough to a wall, activity of these neurons increased from 0 continuously to 1. These sensors were also used to perform low-level obstacle avoidance reflex.

Second, one row of the panoramic camera image was taken as the visual input. The robot was constrained to move in the central portion of the environment, thus the striped wall it sensed by its cameras always remained in a distance serving distal visual cues. To enable the robot to establish its orientation a cue card was simulated. Whenever the robot moved it calculated its orientation relative to the direction of the cue card. The panoramic camera image was then rotated using the robot's self established head direction such that a pixel in a given direction (e.g. the view to the north) was always mapped to approximately the same local visual cell, irrespective of the orientation of the robot. Thus, the reference frame in our case was given by the location of the robot and the direction of the cue card relative to the robot at the beginning of the simulation. Altogether, we simulated 120 visual cells. Firing rate of a visual cell corresponded to the gray scale value of the respective camera pixel normalized in the $[0..1]$ interval.

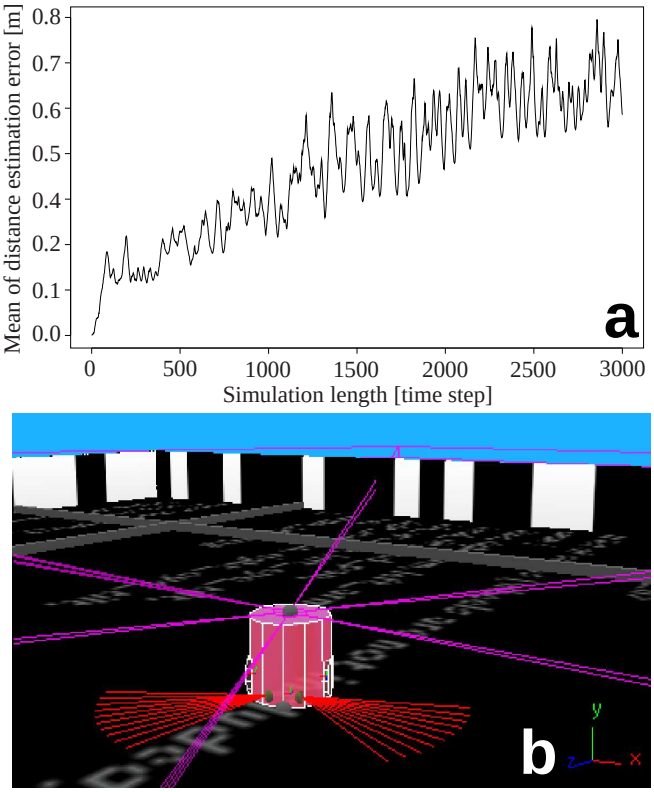

Fig. 2 Properties of the simulation environment. Figure **a** shows the accumulation of noise in the path integration. Error of the location determination based solely on path integration increases as a function of the traveled distance. The line depict the mean difference (δ) between the real position and position calculated from the wheel rotation, each based on 10 independent simulations. Note that in an open arena the increase would correspond to a square root function, however, in our 1x1 meter arena the mean difference is bounded at $\delta_{\max} = 0.521$ meter (Oser et al 1990). Noise strength, $\sigma = 0.05$, see text. Simulation of the model's inputs in Webots (**b**). A simple virtual environment and a mobile robot were simulated. The robot was allowed to wander randomly in the middle part of the environment in a distance from the striped walls. This way we implemented distal visual cues, which were sensed by 6 cameras (lines starting from the top of the robot show the field of vision of each camera) placed on the top of the cylindrical body of the robot generating a panoramic view. Besides the cameras, the robot was equipped with 2·10 distance sensors on its lower portion (lines show their sensitivity range), which served to model whiskers detecting nearby obstacles. Finally, the robot was moved by two wheels, which supplied the proprioceptive input to the neural model by registering their rotation.

Third, the rotation of the differential wheels was registered and a speed vector was calculated serving an input to the entorhinal grid cell system consisting of 270 neurons. The speed vector was considered to be noisy as it is in real animals and robots, giving rise to an inaccurate update of the position's representation by the grid cells, which integrated this noisy speed vector as described in the Sect. 2.4.

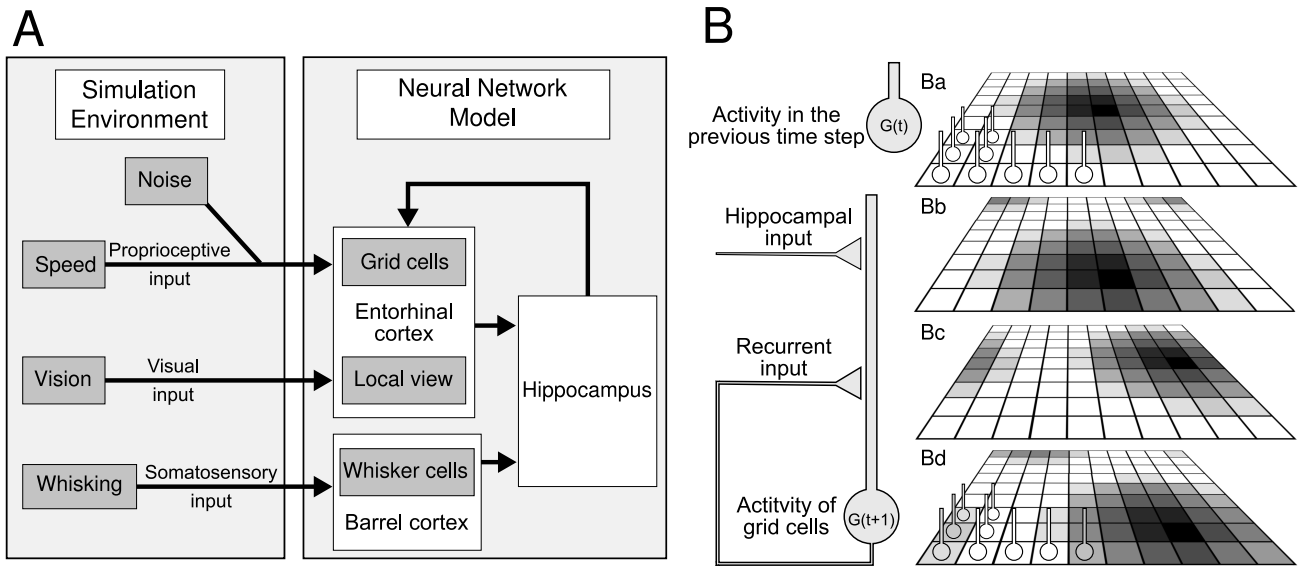

Fig. 1 Overview of the computer model. **A**. The neural network model – consisting of the model of the entorhinal cortical grid cells and local visual cells, whisker cells and the hippocampal place cells – was run in a simulated robot in the Webots environment. Inputs of the model, represented as firing rates of grid, local visual and whisker cells respectively, came from the sensors of the robot sampling a virtual environment. White noise was added to the proprioceptive input (wheel rotation). Neurons in the input layer innervated hippocampal place cells, which in turn fed-back onto the entorhinal grid cells. **B**. The inputs and the activity of the entorhinal grid cells system. Simulated grid cells of a given population receive recurrent inputs from other grid cells of the population and afferent input from the hippocampus, both of which influence the change of grid cell activity in time (left). Grid cells are organized in a matrix, represented in the right panel, where darker color of a square indicates higher grid cell activity. The topology of the recurrent connections initiates the formation of an activity bump (**Ba**) after a few simulation time steps. When the animal moves the noisy proprioceptive input modulates the recurrent connectivity between grid cells and the input of the neurons in the corresponding directions is increased (**Bc**, see Sec. 2.4 and Guanella and Verschure (2006) for more details). The recurrent synaptic (**Bc**) input is integrated with the feed-back input from the hippocampus (**Bb**) and finally the activity bump shifts according to the estimated direction of motion (**Bd**).

The noisy speed was simulated according to the following equation:

$$s' = s * (1 + \xi), \tag{1}$$

where s is the constant noiseless speed measured from the rotation of the robot's wheels, s' is the noisy speed used to update the grid cell system, and ξ is a random variable following the normal distribution with standard deviation σ.

2.3 The simulated hippocampal network and the learning rule

Detailed equations and parameters following our previous work (Ujfalussy et al 2008) describing the implementation of the whisker, local visual and place cells can be found in the Appendix I. The purpose of the hippocampus model in the present simulations was to integrate its inputs and generate a unified representation of the environment by place cells. To achieve this goal we followed the theory proposed by Rolls (1995), which explains how the hippocampal formation operates to serve as an episodic memory device. However, when input patterns are functions of the position, hippocampal cells show place correlated firing activity similar to the behavior of experimentally observed place cells. To achieve this behavior we implemented a Hebbian-like learning algorithm between neurons in the input layer and hippocampal place cells and competition among place cells (Sharp 1991).

2.4 The grid cell model

In a previous version of this model (Ujfalussy et al 2008) grid cells were described by their firing rate, which was implemented as a periodic function of the animal's spatial location, following Blair et al (2007). This simple approach is computationally efficient and allows the simulation of several grid cells at the same time. However, for our present purposes a dynamical description of grid cells is required as we intend to describe the deterioration of the hexagonal spatial firing pattern due to the noisy inputs and the its restoration by modifiable connections between place cells and grid cells. Thus we incorporated the dynamical model of Guanella and Verschure (2006) into our model framework.

This artificial neural network model implements a continuous attractor system on a two dimensional neural space (Fig. 1 **B**). Activity of a neuron is represented by a scalar variable denoting the firing rate of the neuron. The connection among neurons is all-to-all and to return the hexagonal

spatial firing property of grid cells, the connections are implemented on a twisted torus topology of the neural tissue (see Fig. 1 and 2 of Guanella and Verschure (2006)). Starting from a random initial condition, first an activity bump is formed somewhere in the neural space depending on the initial state, which is the stable solution of this continuous attractor system. Integration of the animal's speed – i.e. the displacement of the activity bump – is implemented through the modulation of the connections by shifting them in the direction of the animal's motion. In our simulations we followed the same principle but used the noisy version of the speed vector (Eq. 1).

According to recordings from freely moving rats we used 3 layers of grid cells in the simulations, neurons within each layer sharing a common spacing and all layers had the same orientation (Barry et al 2007). Each layer consisted of 9·10 neurons, each neuron had a different spatial phase. For generating these neurons we used the parameters listed in Table 1, other parameters were kept as in the original paper by Guanella and Verschure (2006).

Parameter	Layer I	Layer II	Layer III
Gain	1	1.5	2
Bias	0	0	0
Spacing [m]	0.80	0.55	0.40

Table 1 Parameters used in our simulations of the grid cell model by Guanella and Verschure (2006). Other parameters were kept as in the original paper. Spacing in the model is a function of the gain parameter.

Additionally to the original model (Guanella and Verschure 2006) calculation of the grid cell activity was modified by the feed-back connections (Fig. 1). Specifically, equation 2 of Guanella and Verschure (2006) was changed into the following form

$$G_i(t) = n\left(n(A_i(t)) + n\left(\sum_{j=1}^{N} W_{ij}^{(\mathbf{H},\mathbf{G})} H_j\right)\right), \quad (2)$$

where A is the original, $\mathbf{G}$ is the modified activity of the grid cells, $\mathbf{H}$ is the rate vector, N is the number of the simulated hippocampal cells, and $n(\cdot)$ is the linear normalization function

$$n(V_i) = \frac{V_i - min(\mathbf{V})}{max(\mathbf{V}) - min(\mathbf{V})} . \quad (3)$$

2.5 Development of the hippocampo-cortical feed-back

In order to study the error correcting capability of the integrated hippocampal place representation we had to adjust the $\mathbf{W}^{(\mathbf{H},\mathbf{G})}$ weight matrix of the feed-back connection projecting from the simulated hippocampal cells to the grid cell population. Each element of the $\mathbf{W}^{(\mathbf{H},\mathbf{G})}$ matrix was initialized to 0. To evolve this matrix three learning rules were used as follows.

The first learning rule we used to modify the hippocampo-cortical feed-back connection was a semi-online rule (termed correlation counting rule). First, during the learning phase, two variables counted the correlated and anti-correlated firing events between all place and grid cell pairs, as described in Table 2 (online phase). Then, when the learning phase was over, we determined the $\mathbf{W}^{(\mathbf{H},\mathbf{G})}$ weight matrix according to the following equation (offline phase):

$$W_{ij}^{(\mathbf{H},\mathbf{G})} = \frac{c}{c+a} . \quad (4)$$

With this rule we could approximate the ratio of the area where the grid cell firing field and the place field overlap and the area of the place field for all i, j pairs, assuming that the robot did a sufficiently fine exploration on the simulation environment during the learning phase. This ratio approximates the probability of grid cell firing given that the presynaptic hippocampal place cell fires. After learning, the $\mathbf{W}^{(\mathbf{H},\mathbf{G})}$ matrix stores these probabilities for each pair.

H_i	G_j	action
$\geq \Theta_{\mathbf{H}}$	$\geq \Theta_{\mathbf{G}}$	$c{+}{+}$
$\geq \Theta_{\mathbf{H}}$	$< \Theta_{\mathbf{G}}$	$a{+}{+}$
$< \Theta_{\mathbf{H}}$	$\geq \Theta_{\mathbf{G}}$	-
$< \Theta_{\mathbf{H}}$	$< \Theta_{\mathbf{G}}$	-

Table 2 Counting of firing events in the correlation counting rule. In case of $A_i > \Theta_{\mathbf{A}}$, the A_i cell was considered to be active, otherwise it was considered to be inactive. c, a: correlation and anti-correlation case counter variables, respectively; and $++$ is the incrementation operator. We used $\Theta_{\mathbf{H}} = 0.3$ and $\Theta_{\mathbf{G}} = 0.6$ values in the simulations.

Table 3 shows the formula of the other two Hebbian-type continuous, on-line learning rules we used: a stabilized Hebb and the presynaptic gating rule (Gerstner and Kistler 2002). The latter is a continuous on-line form of the correlation counting rule, as the synaptic weights converge to the mean firing rate of the grid cells given the presynaptic place cell fires.

Learning rule	Formula
Stabilized Hebb	$\Delta W_{ij}^{(\mathbf{H},\mathbf{G})} = \gamma * \left(H_j * G_i - W_{ij}^{(\mathbf{H},\mathbf{G})}\right)$
Presynaptic gating	$\Delta W_{ij}^{(\mathbf{H},\mathbf{G})} = \gamma * H_j * \left(G_i - W_{ij}^{(\mathbf{H},\mathbf{G})}\right)$

Table 3 The studied continuous learning rules. $\mathbf{H}, \mathbf{G}$: the rate vector of the simulated hippocampal and grid cell populations at the given time step, respectively; γ: learning rate parameter.

Synaptic modification in biological systems implicate intricate, non-linear, time-dependent mechanisms (Bi and Poo 2001). However, in several practical applications involving learning and memory simplified learning algorithms (Gerstner and Kistler 2002) might sufficiently fulfill their role in implementing the necessary functionality. These algorithms usually build on firing activity correlation driven modification of the connectivity matrix and use the Hebbian-type (Hebb 1949) learning rules in a general sense (Arbib 2002). This motivated our above described learning rules as well. Specifically, for the functioning of our proposed mechanism of error correction, the overlap of firing fields of grid and place cells is to be assessed. We suggest that the correlation of temporal firing activity is in accordance with this geometrical property of firing and hence use correlation based learning rules. The most abstract learning rule, the correlation counting rule, is far from a biologically implemented mechanism, however, it is efficient and captures the necessary properties of the required rule in a simple way. The other two rules are more biologically plausible: both come from the family of stabilized Hebb rules, given in general by the formula $\Delta W_{ij}^{(\mathbf{H},\mathbf{G})} = \gamma\left(f(G_i)H_j - g(G_j)W_{ij}^{(\mathbf{H},\mathbf{G})}\right)$ (e.g. see Blais et al (1999)). Specifically, the pre-synaptic gating rule, suggested by Grossberg (Grossberg 1974, 1976a,b) was introduced to describe information processing in the visual cortex of the cat.

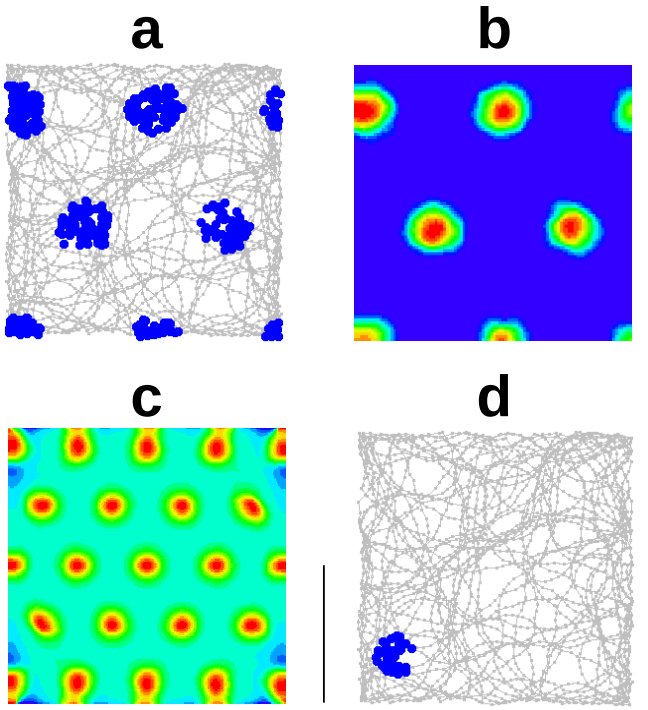

Fig. 3 Spatial activity pattern in the grid and the place cell systems without noise and without hippocampal feed-back. The zig-zagging line on **a** and **d** represent the path of the robot with small black dots at sampling points where sensory information was processed, big dots show where a certain grid or place cell, respectively, had non-zero activity. On **b** the image shows the firing rate map of the same grid cell, and on **c** the spatial auto-correlation function calculated from the rate map. Grid cell parameters were: gain 1.5 and bias 0. The scale bar denotes 0.5 meter for **a**, **b**, and **d** and 1 meter for **c**. Note that in the noiseless situation ideal grid and place codes are generated.

3 Results

3.1 Simulation of the model

Initially, all firing rates and the C_{ij} synaptic matrix elements were set randomly and were modified during the course of the simulation. The $\mathbf{W}^{(\mathbf{H},\mathbf{G})}$ matrix was initialized to 0. To solve the problem of the separation of concurrent learning and exploitation of acquired knowledge, we separated the simulation into two phases as described below.

3.2 Learning phase

During the first (learning) phase of the simulation the cortico-hippocampal connections were modified by Eq. A-4, and the feed-back connections as described in Sect. 2.5. This part of the simulation lasted for 3000 simulation time steps (except for Fig. 6 **b**). During the learning phase, however, the feed-back connections did not influence the activity of the entorhinal grid cells. During this phase the network initialized itself in two ways: First the initially random activity in the grid cell system was stabilized and formed an activity bump due to the attractor dynamics of this subsystem. The bump was formed and path integration started within a few simulation time steps. As noise was turned off initially, grid cells exhibited a robust hexagonal spatial activity pattern (Fig. 3 **a**–**c**).

Second, due to the competition between hippocampal neurons and the self-organizing synaptic modification, input patterns were transformed into a sparse and orthogonal representation in the hippocampus. As described earlier, (Ujfalussy et al 2008) spatially correlated inputs generate place cell activity in the model hippocampus during the learning phase of the simulation (Fig. 3 **d**). Generation of the place code was fast, place fields remain stable after a few visit of a certain location.

An important difference between the previous version of this model (Ujfalussy et al 2008) and its present version is that previously, similarly to other modeling works (Solstad et al 2006; Rolls et al 2006), we used multiple orientations and spacings in the grid cell part of the model. In the present version, however, only one orientation is used and only three spacings, still, integrating the grid input with the visual input results in well expressed place fields in the hippocampus (Fig. 3 **d**).

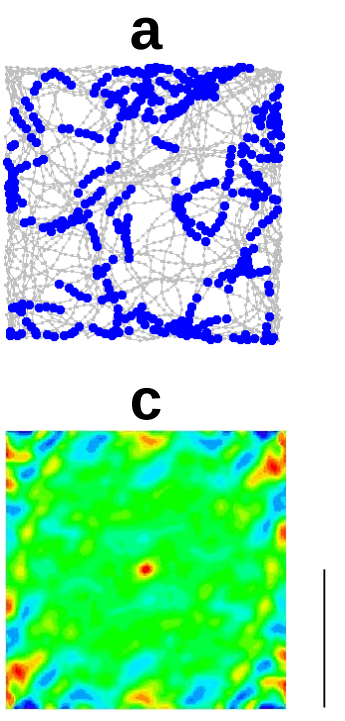

Fig. 4 Spatial activity pattern in the grid and place cell system with noise and without hippocampal feed-back. Placement of subfigures and the cells shown are the same as in Fig. 3. Note that introducing noise in the proprioceptive information distorted the regular firing activity of grid cells. Note that while firing of the place cell became more dispersed, the location of the place field remained similar. The relative usability of the remaining place field is due to the visual part of the input. Noise strength, $\sigma = 0.05$.

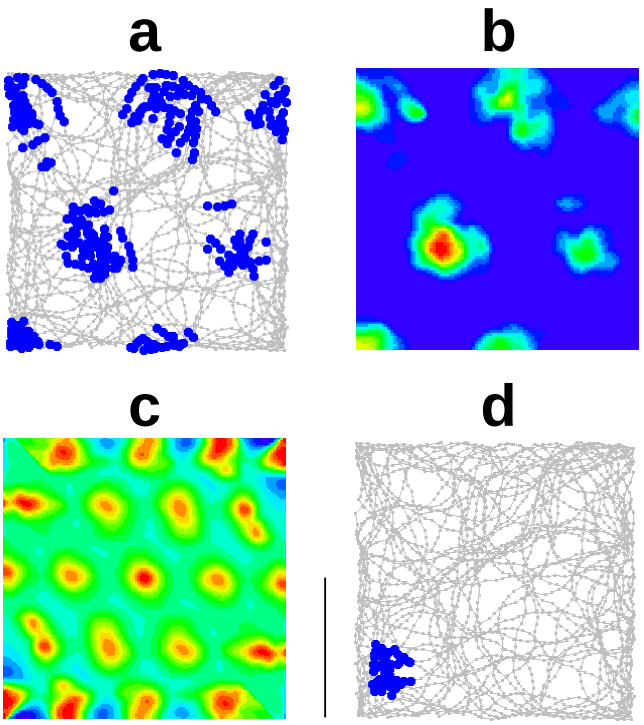

Fig. 5 Spatial activity pattern in the grid and place cell system with noise and hippocampal feed-back. Placement of subfigures and the cells shown are the same as in Fig. 3, noise strength, $\sigma = 0.05$.

3.3 Active feed-back phase

During the second (active feed-back) phase (3000 time steps) synaptic weights did not change and all synaptic pathways influenced their target regions. Also, noise was added to the signal of the rotation sensors of the robot's wheels, which deteriorated the regular activity of the grid system (Fig. 4 **a**–**c**) and invalidated the path integration. As a result, two third of the cortical input vector contained noisy information, which had an impact on the hippocampal place representation, reflected by distorted place fields shown on Fig. 4 **d**.

Simulation results show, however, that activating the hippocampal feed-back resulted in restoring both the grid and the place code (Fig. 5)

3.4 Properties of the hippocampal feed-back innervation

To characterize the error correcting capability of the integrated hippocampal place representation in the grid cell system, we calculated the Pearson correlation at each time point t between the grid activity vector in the noiseless situation ($\mathbf{G}(t)$) and the corrected grid activity when noise was present in the system together with the hippocampo-entorhinal feed-back correction ($\mathbf{G}'(t)$) and averaged for the whole course of the active feed-back phase (3000 time steps):

$$C_X = \langle \mathrm{cor}\left(\mathbf{G}(t), \mathbf{G}'(t)\right)\rangle_{t=[3001..6000]} \quad (5)$$

for all three ($X \in \{\mathrm{I}, \mathrm{II}, \mathrm{III}\}$) grid cell layers (Table 1). This calculation was performed for all three learning rules described in Sect. 2.5 and results were compared in Table 4.

Simulations showed that all three learning rules studied performed equally well. However, when the feed-back excitation was not present the noiseless and the noisy spatial grid patterns were decorrelated. When comparing results obtained for different grid layers (Table 4) we found that the bigger the spacing, the better the error correction. The reason for this can be understood by considering how the correlation counting learning rule works: whenever there is an overlap between the firing field of a grid cell and a place cell a positive correlation was encountered and the synaptic strength matrix element between the corresponding cells was increased. However, when the overlap was only partial and in a given position the place cell was active, but the grid cell was not, an anti-correlation was registered and the corresponding weight matrix element was decreased (Table 2). Increasing the field size of the grid cells would result, on average, in an increased overlap and opens the possibility to reinforce synapses enabling error correction.

In the followings we narrowed down our experiments to the studying of the presynaptic gating learning rule. We next

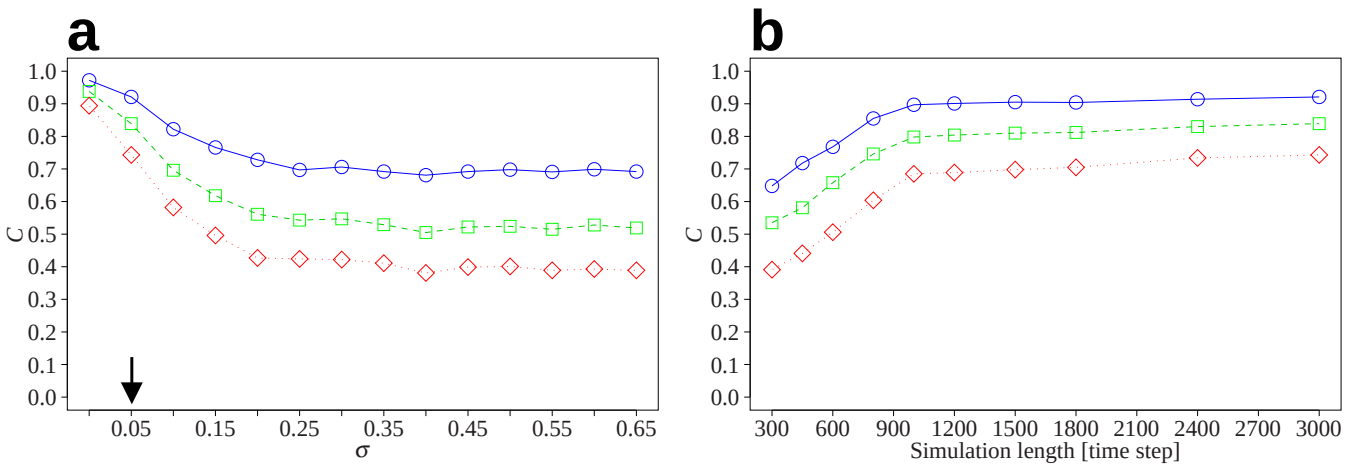

Fig. 6 Error correcting by feed-back. Dependence of the error correcting capability of the presynaptic gating rule, as measured by the correlation described in Eq. 5, on the noise strength (**a**) and on the learning length (**b**). $\sigma = 0.05$ in **b**. Circle – grid layer I, square – grid layer II, diamond – grid layer III. The arrow in **a** indicates the noise strength used in the simulations unless otherwise noted.

Learning rule	C_{I}	C_{II}	C_{III}
Correlation counting	.905	.827	.735
Presynaptic gating	.921	.839	.743
Stabilized Hebb	.921	.838	.742
No feed-back	-.047	.132	-.013

Table 4 Comparison of the three studied learning rules. Calculating and comparing the correlation between the original, noiseless and the corrected grid patterns we found that all three implemented learning rules performed similarly well. However, when the feed-back excitation was turned off the original and the noisy grid patterns were completely decorrelated.

examined the noise tolerance of the feed-back by systematically increasing the σ noise strength parameter and calculating the correlation (Eq. 5). Again, as discussed above, we found that generally grid cell firing patterns with bigger spacings can be better corrected than grids with small spacing (Fig.6 **a**).

Also note that in the $\sigma = 0$ point $C_X(\sigma = 0) < 1$, for all layers. Finite sampling of the environment and different trajectories during the learning and the recall phases lead to an imperfect hippocampal place representation, which, via the feed-back excitation, influenced the grid system even in the noiseless case. Overall, we found that increasing the sensory noise up to about $\sigma = 0.2$, the error correction performance of the feed-back decreased until it reached a limit value, which was different for each grid layer, however, further increasing the noise would not result in a significant drop of the performance: Above a critical noise level, the information in the proprioceptive input was negligible compared to the allothetic inputs. We also found that depending on ratio of the number of grid cells, and visual cells, – i.e. the ratio between noisy and noiseless inputs – the limit varies: the less noisy input cells included, the better the error correction (data not shown).

Next, we examined how the length of the learning phase influences the error correction potential of the feed-back. To create comparable results, the simulation was divided into three parts: first, the robot was engaged in learning for some time steps (τ_{l}); second, it continued its random walk without any modification of the synapses for some more time steps (τ_0) such that $\tau_{\mathrm{l}} + \tau_0 = 3000$; third the active feed-back phase begun and lasted for $\tau_{\mathrm{a}} = 3000$ time steps. This way, we ensured that in the active feed-back stage the robot traveled along the same path.

Simulation results on the learning length (Fig. 6 **b**) indicated that approximately 700 time steps were sufficient in our situation to reach the asymptotic value of the correlation used to measure error correction. There are two basic processes that influence the length of the learning: first, the feed-back synaptic matrix is modified to associate hippocampal cell firing with grid cell firing. We found that in the examined parameter interval ($\gamma = [0.1 \,..\, 0.5]$) the learning rate did not effect overall learning time (data not shown). Second, the robot had to sample the environment long enough, such that it was able to form enough associations between hippocampal and grid fields when visiting a certain place. Indeed, while the robot traversed place fields that were not associated to grid fields by the feed-back during learning, the path integrator run free of the hippocampal influence, thus accumulated the sensory noise. Fig. 7 shows the time evolution of the above described error correction.

On the whole, we found that after the sufficient amount of learning was accomplished (about 700 time steps in our case) error correction in the grid cell system took place and an appropriate place representation was generated.

3.5 Predictions of the model

We studied the properties of the simulated grid cell – place cell system in situations when the environment around the robot changes. In the first set of experiments we tested how

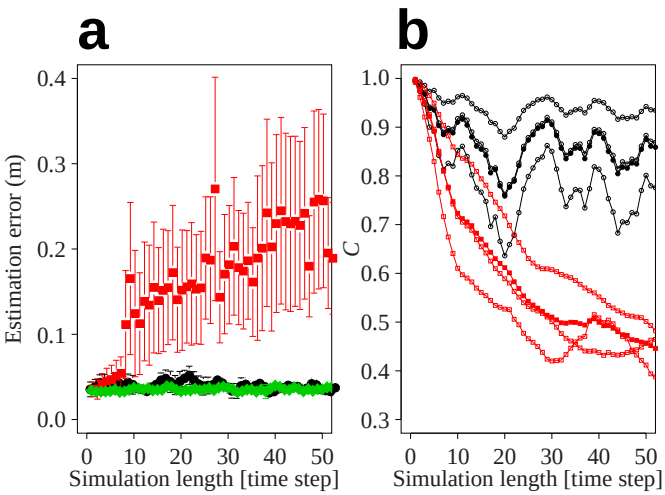

Fig. 7 Continuous error correction by feed-back. **a** Estimation of the robot's position based on the grid system (see Appendix II). Symbols show mean, error bars SEM of the position without error correcting feed-back (red, squares), with feed-back (black, diamonds) and without noise (green, dots). **b** Error accumulation in the grid cell system quantified by the correlation between different realizations of the grid-system (see Eq. 5). Open red squares represent the correlation of the noise-free grid-system with the noisy system without hippocampal feed-back for the three simulated grid layers. Open black circles denote correlations of the noise-free system with the noisy system, when its activity is corrected by the hippocampal feed-back, given for the three layers of the grid-system. Filled symbols represent the mean for the three layers. This figure is based on the average of ten runs. See text for details.

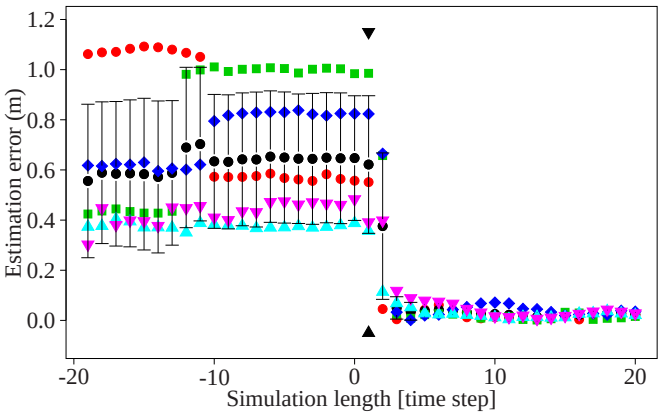

Fig. 8 Recovery after disorientation. See text for the protocol used. The five symbols show position estimation values (see Appendix II) for five runs, the symbols with the error bars show their average and standard deviation. The black arrows at time step 1 indicates when the visual input was turned back on. Note the instantaneous improvement of the position estimation after visual correction of the ongoing activity.

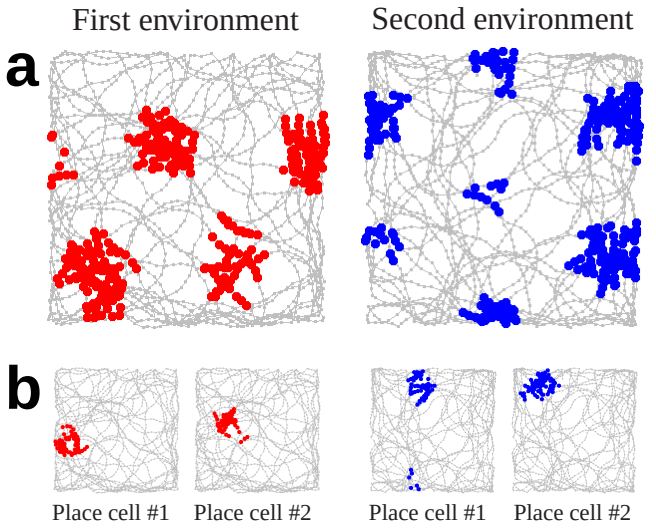

Fig. 9 Remapping in a new environment. Left column: first environment, right column: second environment. Figure **a** shows a selected grid cell, and **b** two place cells in the first and in the second environment, respectively. For details see the text.

the grid- and place cell systems are able to identify the location of the robot in an already learned, familiar, environment after disorientation (Fig. 8). For this experiment, the robot first learned positions in the environment for 3000 time steps. Then, the grid activity was randomized and the robot wandered from a random starting point for 200 time steps with the visual input turned off. Third, the visual input was turned back on, and the robot kept wandering for 200 time steps.

As shown on Fig. 8 after the visual input is turned back (black arrows), the estimation of the robot's position based on the grid cell system (see Appendix II for the methodology) or the place cell system (data not shown) rapidly improves, showing that the grid cell system and the place cell system runs in accordance with the previously learned pattern, i.e. the robot is able to recover from a disorientation and recognizes an already visited environment.

In a second set of experiments the robot was put into a novel environment. Specifically, the robot was first put into an environment and learned the locations as described in Sect. 3.2. After learning in the first environment the striped pattern on the walls was changed to simulate a new environment and the robot was allowed to learn again for 3000 time steps. After learning spatial receptive fields of grid and place cells were evaluated (Fig. 9).

We found that grid cells remap coherently, as expected. Any two grid cells will preserve their relative phase, each grid cell will have the same spacing and their orientation change the same degree, in accordance with experimental observations (Fyhn et al 2007).

Place cells perform global remapping. Some place cells were only active in one of the environments (approximately 40% of the cells in the first only, about 30% in the second only), some in both (about 10%) and some remained silent in both. Place fields of those cells that were active in both environment were independent. We also found that place fields in the second environment were slightly larger than in the first (data not shown). These observations can be explained by taking into account the competitive learning mechanism used in the hippocampal system. Cells that learned to represent a certain location will have synaptic strength associated to them such that only the input pattern describing the loca-

tion of their place field will activate them, thus in the new environment they will not be able to learn. Naive cells, which were not involved in the representation of the first environment, on the other hand, will be able to learn places. Also, as in the second environment less cells are able to learn, their resulting place field will be bigger.

Finally, to explicitly test how visual and proprioceptive inputs are combined, in a third set of experiments we simulated the morphing of the environment. The oversimplified visual system used in the model did not allow us to simply stretch the arena together with the striped pattern on its wall because in this case the robot did not recognize the distorted visual input.

However, to simulate the conflict between the visual and the proprioceptive system, we developed an other method. During the learning phase the gain parameter (see Table 1) of the grid cell system was modified, while the environment was kept unchanged. During the active feed-back phase, the gain parameter was set back to its original value, thus simulating a mismatch between the proprioceptive and the visual inputs. Specifically, the gain parameter of the grid cells was changed from 1 to 1.5 in the vertical direction and kept 1 in the horizontal direction for learning. As a result, during learning the hippocampal feed-back was associated with a distorted grid pattern that moved 1.5 times faster in the vertical direction than in the horizontal direction. During recall the gain parameter in the vertical direction was set back to 1, simulating that the side of the arena corresponding to the vertical direction was shortened 1.5 times while the visual cues remained unchanged. Without hippocampal feed-back, the grid activity exhibited the regular hexagonal pattern according to its proprioceptive input (Fig. 10 **a**). However, when the hippocampal feed-back was turned on, the grid pattern was compressed 1.5 times in the vertical direction (Fig. 10 **b**). During recall, the hippocampal feed-back forced the grid activity to change faster in the vertical direction, due to the associations learned previously, resulting in the compressed grid pattern.

Thus we conclude, that the visual input is able to continuously influence the entorhinal path integrator system via an integrated hippocampal place representation.

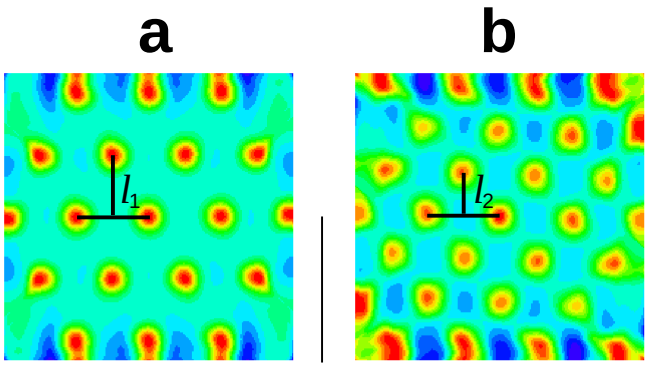

Fig. 10 Effect of scaling the proprioceptive input relative to the visual input on the grid cell activity. The spatial autocorrelation function of one representative grid cell is shown without (**a**) and with (**b**) hippocampal feed-back. During learning a vertically compressed grid cell activity were associated with the hippocampal place representation. As shown on figure **a**, after rescaling the proprioceptive input during recall, the regular hexagonal spatial firing pattern of grid cells were reestablished in the absence of hippocampal feed-back. However, figure **b** shows that the visual input induce vertical rescaling in the grid cell system via the hippocampal feed-back. The magnitude of the vertical rescaling ($\frac{l_1}{l_2} = 1.5$) was exactly the same as modulation of the corresponding gain parameter.

4 Discussion

We have analyzed a computer model of the rodent cortico-hippocampal system from the perspective of place learning and recognition as a continuation of our previous work (Ujfalussy et al 2008). The main result of our study is that a representation of locations integrating visual and proprioceptive information can be used to decrease the harmful effect of sensory noise accumulating in the path integrator subsystem. Specifically, we have shown that although the noisy self locomotion information would distort the firing pattern of entorhinal cortical grid cells a feed-back excitation from hippocampal place cells can restore the correct pattern and at the same time improve the properties of place fields themselves as well, in a circularly causal manner.

Based on experimental evidence (Wilson and McNaughton 1993) in a theoretical framework McNaughton et al (1996) proposed that the visual information might be used both to establish the initial location of rodents – initialize its path integrator system – and to correct for accumulating error. Following this idea, there have been attempts to explain how a stable representation in the path integrator system might emerge. For example, Arleo and Gerstner (2000) have presented a model in which they define abstract extra-hippocampal path integrator neurons (in fact, rather similar to grid cells found five years later), which integrated wheel rotation. They also faced the problem of accumulating error and used visual cues to eliminate its harmful effect. Namely, after a certain amount of time their robot stopped exploration and searched for familiar visual cues. When a cue was found to be reliable enough the path integrator was reset to the current location determined by the visual stimulus.

Our model fits in this general theory as it uses the visual information to correct path integration (we hypothesize that olfactory, auditory or whisking inputs could also be used for this corrections as these modalities are similar to vision in that noise does not cause error to accumulate in their representations). However, in our model not only the visual, but the integrated (visual & proprioceptive) information was used to correct the path integration error (c.f. (O'Keefe and Burgess 2005)). Moreover, we did not introduce discrete time points or set up thresholds when a recalibration becomes necessary, instead building on the anatomy of the hippocampus (Amaral and Witter 1989) and implementing the modifiable hippocampo-cortical feed-back, continuously corrected the path integrator. This continuous in-

fluence of allothetic information on the path integration system is supported by the fact that entorhinal grid cells' firing fields rescaled in response to environmental deformation (Barry et al 2007).

Theories on the hippocampo-cortical feed-back mostly hypothesize on its functional role in respect of the episodic memory aspect of the cortico-hippocampal system (Treves and Rolls 1994; Lőrincz and Buzsáki 2000; Witter et al 2000). According to these theories the hippocampus is able to rapidly form a new representation upon passing through a new episode e.g., visiting an unknown location. After the memories are formed the feed-back activation could provide information useful to the neocortex in the building of new representations by recalling previous memories, which process would constitute a form of memory consolidation (Rolls and Kesner 2006). Also, a closed loop connecting layer II-III of the entorhinal cortex to the hippocampus and from the latter to the deep layers of the entorhinal cortex (Witter et al 2000) might serve to continuously compare new inputs and temporarily stored information in order to facilitate the decision whether a new or an already stored experience is encountered.

An other aspect of the feed-back connection might be that when only a fragment of the episode is presented, it is able to recall the whole episodic memory through the back-projection pathways from the hippocampus to the cerebral neocortex, resulting in reinstatement of neuronal activity in association areas of the cerebral neocortex similar to that present during the original episode (Treves and Rolls 1994). Similarly, in our model the location of the animal can be continually recalled based on visual cues. Conversely, in the absence of vision (e.g., in darkness) the animal could retrieve visual landmarks associated with its location based on its position information coming from path integration.

The model proposed by Gaussier et al (2007) suggests a different role for the hippocampo-entorhinal feed-back, including an explanation of spatially correlated processes as well. In this model there is again a continuous interplay between the hippocampus and the entorhinal cortex, where the latter stores and recognizes input configurations, while the former identifies transitions from the present towards new states. This approach is somewhat similar to ours in that the entorhinal grid cell system is partly driven by the hippocampus, but differs in that Gaussier et al (2007) do not assume attractor dynamics as the basis for the generation of grid cells but suppose that the operation of an extra-hippocampal system endowed with "long-distance" path integration capabilities creates the grid activity in the entorhinal cortex given some properties of the connections between the two structures.

In our model, the representation of the anatomy of the entorhinal cortex and the hippocampal feed-back is not detailed. It is known, however, that the hippocampus sends afferents to the deep layers of the entorhinal cortex and receives efferents from the superficial layers (Witter et al 2000). It is also known, that classical grid cells can primarily be found in layer II of the EC, while deeper layers (III, V, and VI) contain grid cells, head-direction cells and conjunctive grid and head-direction cells (Sargolini et al 2007). Interestingly, there is an extensive system of connections among entorhinal cortical layers too (van Haeften et al 2003; Kloosterman et al 2003), which implicates that the grid representation and the path integration in the entorhino-hippocampal system is an emergent property, which requires all participating regions and layers. Intriguingly, the head-direction system, which likely originates in the lateral mammillary nucleus, reaches the entorhinal cortex via the postsubiculum and innervates its superficial layers (Taube 2007). Adding to the similarity between the grid-system and the hippocampal place-system is the fact, that the entorhinal cortex innervates the mammillary nuclei (Shibata 1988). Within our model framework, we propose an overall functional role of the hippocampal feed-back, without a detailed explanation of the precise connection structure.

In the presented model we used the approximation that noise in the proprioceptive input was only simulated when the synaptic connections were already established. This is due to the fact that we primarily intended to show that an integrated place representation can be used to correct one of its constituent part. The learning process was necessary to set the appropriate weight matrix for the feed-back connection. However, we propose that the shown mechanism can be utilized by animals as well, considering their exploratory strategy. Animals (from arthropods to rodents) were shown to start the exploration of a new environment by short trips, initially frequently returning to their nest or an other initial location (Collett and Zeil 1998; Etienne et al 1998) and move further away only after they are familiar with their immediate surrounding. This exploration strategy is in favor of our proposed model as during the short trips only small error accumulates in the path integrator. If the learning process lasts only for a short time – and our simulation results showed that a learning converges rapidly –, and after learning the feed-back is used to correct the path integrator, than with a gradual exploration and learning the animal is able to enlarge its map while keeping the hippocampus and entorhinal cortex always in register.

Theoretically, the allothetic information could reach the path integrator system directly, or indirectly through an integrated representation from the hippocampus. Manipulations resulting from a coordinated alteration of both the hippocampal and the entorhinal representations like rotation of the environmental landmarks (Hafting et al 2005), deformation of the enclosure (Barry et al 2007) or induction of simultaneous global remapping in the hippocampus and grid cell realignment (Fyhn et al 2007) can be interpreted within both the direct and the indirect framework. Our model predict, however, that after the inactivation of the hippocampus, firing of grid cells would remain location dependent but would become more dispersed and would not follow environmental manipulations. Indeed, recordings on a linear track showed that although hippocampal inactivation did not disrupt the spatially confined firing of the grid cells, the fields became wider and less stable (Hafting et al 2008) supposedly be-

cause of the accumulating error in the path integrator system.

In our simulations the hexagonal firing pattern of the grid cells was generated by an attractor network of entorhinal neurons that requires specific connectivity pattern (Guanella and Verschure 2006; McNaughton et al 2006; Fuhs and Touretzky 2006). Our basic idea, that allothetic information reaches the grid cells indirectly though the hippocampus can also be used in an other class of grid cell models (Hasselmo et al 2007; Burgess et al 2007), where grid cell firing arises from interference of theta frequency membrane potential oscillations in single neurons. In this case, hippocampal place cells should continually reset the phase of the dendritic oscillations of entorhinal grid cells. Spike timing dependent plasticity rules during exploration could be used to set up the proper connectivity (Lengyel et al 2005). Hippocampal and entorhinal phase precession (Hafting et al 2008) and subthreshold oscillation of entorhinal grid cells (Giocomo et al 2007) support this scenario.

APPENDIX I

This Appendix summarizes the technical details of the paper Ujfalussy et al (2008) about the hippocampal network, part of the neural network model described here (Fig. 1). In the present model we simulated 1000 hippocampal cells described by a rate vector **H**. These cells were innervated by neurons of the input layer (described by the rate vector **I**) consisting of grid cells (**G**), local view cells and whisker cells, but not by other hippocampal cells. The simulation was divided into two phases (Rolls 1995), learning and active feed-back, respectively.

During the learning phase (Sect. 3.2) first, the afferent innervation from the input layer was used to calculate the activation (**h**) of hippocampal neurons

$$h_j = \sum_i C_{ij} I_i, \tag{A-1}$$

where C_{ij} describes the strength of each synapse between the input layer and the hippocampus. Second, from the activation vector firing rates were calculated using a nonlinear activation function $f(\cdot)$

$$\mathbf{H} = f(\mathbf{h}, \chi), \tag{A-2}$$

where χ is the desired sparseness of the coding and **h** is the hippocampal activation vector. The function $f(\cdot)$ was implemented by an iteration, which selected the most active neurons and scaled their activation into the $[0\,..\,1]$ interval such that the desired sparseness χ was reached:

$$\frac{<\mathbf{H}>^2}{<\mathbf{H}^2>} \stackrel{!}{=} \chi \tag{A-3}$$

During learning the connection matrix (C_{ij}) was modified by a Hebbian-type learning rule

$$\Delta C_{ij} = \alpha H_j (I_i - C_{ij}), \tag{A-4}$$

where α is the learning rate.

During the active feed-back phase (Sect. 3.3) cell activities were calculated by the same set of equations A-1 – A-3, but C_{ij} was fixed.

In the simulations all-to-all connections were applied in C_{ij}. Initial matrix elements were picked from a normal distribution:

$$P(C_{ij} = w) = \frac{1}{\sqrt{2\pi}\rho} \mathrm{e}^{-\frac{(w-\mu)}{2\rho^2}}, \quad \text{if } 0 < w < 1 \tag{A-5}$$

Table 5 lists parameters used in the hippocampal model.

Parameter	Value	Description
N	1000	Number of cells
α	0.05	Learning rate
χ	0.01	Sparseness of coding
μ	0.6	Mean synaptic strength
ρ	0.1	Deviation of synaptic strengths from mean

Table 5 Default parameter values used in simulations of the hippocampal model

APPENDIX II

This Appendix describes calculation of the robot's estimated position based on the firing of grid or place cells. We quantified the efficiency of the hippocampal feed-back by estimating the location of the robot based on the activity of the grid cells. First, we calculated the two dimensional firing rate map of each grid cell during the learning period. Second, we obtained a probabilistic robot location map by multiplying point-wise the rate maps of all simultaneously active grid cells during the recall period. Finally, the maximum of this map gave us a rough estimation of the current position of the robot. This measure was used in Figures 7 and 8.

Acknowledgements Authors are grateful for the useful discussions held at the Budapest Computational Neuroscience Forum organized by Máté Lengyel. The research was funded by the EU Framework 6 ICEA project (IST 027819).

References

Amaral DG, Lavenex P (2006) The Hippocampus Book, Oxford University Press, chap 3. Hippocampal Neuroanatomy

Amaral DG, Witter MP (1989) The three dimensional organization of the hippocampal formation: a review of anatomical data. Neuroscience 31:571–591

Arbib MA (ed) (2002) The Handbook of Brain Theory and Neural Networks, 2nd edn, The MIT Press, Cambridge, MA, chap Post-Hebbian Learning Algorithms, pp 533–539

Arleo A, Gerstner W (2000) Spatial cognition and neuro-mimetic navigation: a model of hippocampal place cell activity. Biological Cybernetics 83:287–299

Barry C, Burgess N (2007) Learning in a geometric model of place cell firing. Hippocampus 17:786–800

Barry C, Lever C, Hayman R, Hartley T, Burton S, O'Keefe J, Jeffery K, Burgess N (2006) The boundary vector cell model of place cell firing and spatial memory. Reviews in the Neurosciences 17:71–97

Barry C, Hayman R, Burgess N, Jeffery KJ (2007) Experience-dependent rescaling of entorhinal grids. Nature Neuroscience 10:682–684

Bi Gq, Poo Mm (2001) Synapticmodification by correlated activity: Hebb's postulate revisited. Annual Review of Neuroscience 24:139–166

Blair HT, Welday AC, Zhang K (2007) Scale-invariant memory representations emerge from moiré interference between grid fields that produce theta oscillations: a computational model. Journal of Neuroscience 27:3211–3229

Blais BS, Shouval HZ, Cooper LN (1999) The role of presynaptic activity in monocular deprivation: Comparison of homosynaptic and heterosynaptic mechanisms. Proceedings of the National Academy of Sciences of the United States of America 96(3):1083–1084

Burgess N, O'Keefe J (1996) Neuronal computations underlying the firing of place cells and their role in navigation. Hippocampus 6:749–762

Burgess N, Recce M, O'Keefe J (1994) A model of hippocampal function. Neural Networks 7:1065–1081

Burgess N, Jackson A, Hartley T, O'Keefe J (2000) Predictions derived from modelling the hippocampal role in navigation. Biological Cybernetics 83(3):301–312

Burgess N, Barry C, O'Keefe J (2007) An oscillatory interference model of grid cell firing. Hippocampus 17(9):801–812

Collett T, Zeil J (1998) Places and landmarks: an arthropod perspective. In: Healy S (ed) Spatial representation in animals, Oxford University Press, pp 18–53

Etienne AS, Jeffery KJ (2004) Path integration in mammals. Hippocampus 14:180–192

Etienne AS, Maurer R, Séguinot V (1996) Path integration in mammals and its interaction with visual landmarks. Journal of Experimental Biology 199:201–209

Etienne AS, Berlie J, Georgakopoulos J, Maurer R (1998) Role of dead reckoning in navigation. In: Healy S (ed) Spatial representation in animals, Oxford University Press, pp 54–68

Fuhs MC, Touretzky DS (2006) A spin glass model of path integration in rat medial entorhinal cortex. Journal of Neuroscience 26:4266–4276

Fyhn M, Hafting T, Treves A, Moser MB, Moser EI (2007) Hippocampal remapping and grid realignment in entorhinal cortex. Nature 446:190–194

Gaussier P, Banquet JP, Sargolini F, Giovannangeli C, Save E, Poucet B (2007) A model of grid cells involving extra hippocampal path integration, and the hippocampal loop. Journal of Integrative Neuroscience 6:447–476

Gerstner W, Kistler W (2002) Spiking Neuron Models. Cambridge University Press, URL http://icwww.epfl.ch/˜gerstner/SPNM

Giocomo L, Zilli E, Fransen E, Hasselmo M (2007) Temporal frequency of subthreshold oscillations scales with entorhinal grid cell field spacing. Science 315(5819):1719–1722

Gothard KM, Skaggs WE, McNaughton BL (1996) Dynamics of mismatch correction in the hippocampal ensemble code for space: Interaction between path integration and environmental cues. Journal of Neuroscience 16:8027–8040

Grossberg S (1974) Classical and instrumental conditioning by neural networks. Progress in Theoretical Biology 3:51–141

Grossberg S (1976a) Adaptive pattern classification and universal recoding I: Parallel development and coding of neural feature detectors. Biological Cybernetics 23:121–134

Grossberg S (1976b) Adaptive pattern classification and universal recoding II: Feedback, expectation, olfaction, and illusions. Biological Cybernetics 23:187–202

Guanella A, Verschure PFMJ (2006) A model of grid cells based on a path integration mechanism. In: Kollias S, Stafylopatis A, Duch W, Oja E (eds) Artificial Neural Networks – ICANN 2006, Springer-Verlag Berlin Heildelberg, Lecture Notes in Computer Science, vol 4131, pp 740–749

van Haeften T, Baks-te-Bulte L, Goede PH, Wouterlood FG, Witter MP (2003) Morphological and numerical analysis of synaptic interactions between neurons in deep and superficial layers of the entorhinal cortex of the rat. Hippocampus 13:943–952

Hafting T, Fyhn M, Molden S, Moser MB, Moser EI (2005) Microstructure of a spatial map in the entorhinal cortex. Nature 436:801–806

Hafting T, Fyhn M, Bonnevie T, Moser MB, Moser EI (2008) Hippocampus-independent phase precession in entorhinal grid cells. Nature 453(7199):1248–1252

Hasselmo M, Giocomo L, Zilli E (2007) Grid cell firing may arise from interference of theta frequency membrane potential oscillations in single neurons. Hippocampus 17(12):1252–1271

Hebb DO (1949) The organization of behavior. Wiley, New York

Jeffery KJ (1998) Learning of landmark stability and instability by hippocampal place cells. Neuropharmacology 37:677–687

Jeffery KJ (2007) Integration of the sensory inputs to place cells: What, where, why, and how? Hippocampus 17:775–785

Jeffery KJ, O'Keefe J (1999) Learned interaction of visual and idiothetic cues in the control of place field orientation. Experimental Brain Research 127:151–161

Kloosterman F, Van Haeften T, Witter MP, Lopes Da Silva FH (2003) Electrophysiological characterization of interlaminar entorhinal connections: an essential link for re-entrance in the hippocampal-entorhinal system. European Journal of Neuroscience 18:3037–3052

Knierim JJ, Kudrimoti HS, McNaughton BL (1995) Place cells, head direction cells, and the learning of landmark stability. Journal of Neuroscience 15:1648–1659

Lengyel M, Kwag J, Paulsen O, Dayan P (2005) Matching storage and recall: hippocampal spike timing-dependent plasticity and phase response curves. Nature Neuroscience 8(12):1677–1683

Leutgeb JK, Leutgeb S, Moser MB, Moser EI (2007) Pattern separation in the dentate gyrus and CA3 of the hippocampus. Science 315:961–966

Lőrincz A, Buzsáki G (2000) Two-phase computational model training long-term memories in the entorhinal-hippocampal region. Annals of the New York Academy of Sciences 911:83–111

Maaswinkel H, Whishaw IQ (1999) Homing with locale, taxon, and dead reckoning strategies by foraging rats: sensory hierarchy in spatial navigation. Behavioural Brain Research 99:143–152

McNaughton BL, Barnes C, Gerrard J, Gothard K, Jung M, Knierim J, Kudrimoti H, Qin Y, Skaggs W, Suster M, Weaver K (1996) Deciphering the hippocampal polyglot: the hippocampus as a path integration system. Journal of Experimental Biology 199:173–185

McNaughton BL, Battaglia FP, Jensen O, Moser EI, Moser MB (2006) Path integration and the neural basis of the 'cognitive map'. Nature Reviews Neurosciences 7:663–678

Michel O (2004) Webots: Professional mobile robot simulation. Journal of Advanced Robotics Systems 1(1):39–42, URL http://www.ars-journal.com/ars/SubscriberArea/Volume1/39-42.pdf

Muller RU, Kubie JL (1987) The effects of changes in the environment on the spatial firing of hippocampal complex-spike cells. Journal of Neuroscience 7:1951–1968

Nardini M, Jones P, Bedford R, Braddick O (2008) Development of cue integration in human navigation. Current Biology 18:689–693

O'Keefe J, Burgess N (2005) Dual phase and rate coding in hippocampal place cells: theoretical significance and relationship to entorhinal grid cells. Hippocampus 15:853–866

O'Keefe J, Dostrovsky J (1971) The hippocampus as a spatial map. preliminary evidence from unit activity in the freely-moving rat. Brain Research 34:171–175

O'Keefe J, Nadel L (1978) The Hippocampus as a Cognitive Map. Oxford University Press, URL http://www.cognitivemap.net/

Oser HJ, Murchland JD, Daley DJ, Vaughan RJ (1990) An average distance. In: Klamkin MS (ed) Problems in Applied Mathematics: Selections from SIAM Review, Society for Industrial Mathematics, Philaderphia, pp 76–79

R Development Core Team (2007) R: A Language and Environment for Statistical Computing. R Foundation for Statistical Computing, Vienna, Austria, URL http://www.R-project.org, ISBN 3-900051-07-0

Rolls ET (1995) A model of the operation of the hippocampus and entorhinal cortex in memory. International Journal of Neural Systems 6:51–71

Rolls ET, Kesner RP (2006) A computational theory of hippocampal function, and empirical tests of the theory. Progress in Neurobiology 79:1–48

Rolls ET, Stringer SM, Elliot T (2006) Entorhinal cortex grid cells can map to hippocampal place cells by competitive learning. Network 17:447–465

Sargolini F, Fyhn M, Hafting T, McNaughton BL, Witter MP, Moser MB, Moser EI (2007) Conjunctive representation of position, direction, and velocity in entorhinal cortex. Science 312:758–762

Séguinot V, Maurer R, Etienne AS (1993) Dead reckoning in a small mammal: the evaluation of distance. Journal of Comparative Physiology A 173:103–113

Sharp PE (1991) Computer simulation of hippocampal place cells. Psychobiology 19(2):103–115

Shibata H (1988) A direct projection from the entorhinal cortex to the mammillary nuclei in the rat. Neuroscience Letters 90:6–10
Solstad T, Moser EI, Einevoll GT (2006) From grid cells to place cells: a mathematical model. Hippocampus 16:1026–1031
Solstad T, Boccara CN, Kropff E, Moser MB, Moser EI (2008) Representation of geometric borders in the entorhinal cortex. Science 19(5909):1865–1868
Taube JS (2007) The head direction signal: Origins and sensory-motor integration. Annual Review of Neuroscience 30:181–207
Touretzky DS, Redish AD (1996) Theory of rodent navigation based on interacting representations of space. Hippocampus 6(3):247–270
Treves A, Rolls ET (1994) Computational analysis of the role of the hippocampus in memory. Hippocampus 4:374–391
Ujfalussy B, Erős P, Somogyvári Z, Kiss T (2008) Episodes in space: A modelling study of hippocampal place representation. In: Asada M, Hallam JCT, Meyer JA, Tani J (eds) From animals to animats, ISAB, Springer, Lecture Notes in Artificial Intelligence, vol 5040, pp 123–136
Wiener SI, Korshunov VA, Garcia R, A B (1995) Inertial, substratal and landmark cue control of hippocampal CA1 place cell activity. European Journal of Neuroscience 7:2206–2219
Wilson MA, McNaughton BL (1993) Dynamics of the hippocampal ensemble code for space. Science 261:1055–1058
Witter MP, Naber PA, van Haeften T, Machielsen WCM, Rombouts SARB, Barkhof F, Scheltens P, Lopes da Silva FH (2000) Cortico-hippocampal communication by way of parallel parahippocampal-subicular pathways. Hippocampus 10:398–410
Zipser D (1985) A computational model of hippocampal place fields. Behavioral Neuroscience 99(5):1006–1018